Congestion and Position Aware Dynamic Routing for the Internet of Vehicles

Ruiyan Han, Quansheng Guan, *Senior Member, IEEE*, F. Richard Yu, *Fellow, IEEE*, Jinglun Shi, and Fei Ji, *Member, IEEE*

***Abstract*—The coupling of packet forwarding, Internet gateway (IGW) selection, and vehicle mobility in the Internet of Vehicles (IoV) presents challenges for multi-hop routing. Particularly, IGWs and vehicles near IGWs are most likely to be congested, since all the Internet traffic loads converge at IGWs in IoV. To this end, we propose a distance-weighted back-pressure dynamic routing (DBDR), which prioritizes the vehicles that are close to the destination and have a large backlog differential of buffer queues to provide dynamic hop-by-hop forwarding. DBDR is also jointly designed with multi-hop IGW discovery and vehicle mobility management to implement both uplink and downlink forwarding for Internet services. Our analysis using Lyapunov drift theory proves that DBDR achieves the network stability on the buffer queues and the network capacity. Simulations in a practical road scenario using NS-2 and VanetMobiSim show that DBDR outperforms the existing protocols in terms of packet delivery ratio, throughput, and success rate of HTTP requests/responses, as well as average packet delay when the network becomes congested.**

***Index Terms*—Back pressure, dynamic routing, Internet of Vehicles (IoV), lyapunov drift, vehicular ad hoc networks (VANETs).**

I. Introduction

THE vision of future intelligent transportation system (ITS) demands connecting and controlling vehicles via the Internet. Vehicles also need the Internet access to enjoy mobile Internet services, such as content download, media streaming and social networking, etc. [1]–[3]. Thus, the Internet of vehicles (IoV) becomes an emerging concept that integrates vehicle ad hoc networks (VANETs) with Internet of things (IoT) [4]. Vehicles connect to the Internet by communicating with the Internet gateway (IGW) through the fixed Roadside Units (RSUs) [5]–[11]. In IoV, RSUs are installed at fixed position and often serve also as IGWs, typically equipped with both wired and wireless interfaces to connect both the Internet and the vehicular network. Considering the scarce deployment of RSUs, vehicles are often far away from RSUs. Internet request/response packets have to be forwarded by multiple hops between vehicles and RSUs using both vehicle-to-infrastructure (V2I) communications and vehicle-to-vehicle (V2V) communications [12].

Multi-hop routing in IoV is different from that in VANETs. Both the origin and the destination of traffic are vehicles in VANETs. However, vehicles will establish a bi-directional IP connection with the Internet in IoV. The IP connection in IoV has to consider jointly gateway discovery/selection and vehicle mobility management together with multi-hop routing. Thus, the unique characteristics of IoV present many challenges on multi-hop routing.

Firstly, the high moving speed of vehicles will result in dynamically changing topology and frequently interrupt the forwarding path between a vehicle and an IGW. In this case, it is almost impossible to maintain a fixed forwarding path for the Internet traffic. IoV demands a dynamic routing due to the fast moving vehicles. Secondly, IGW and vehicles that are close to IGWs may become hot-spots in the network. As a bridge for vehicles and the Internet in IoV, the Internet traffic will converge at IGWs. Vehicles near IGWs are possibly selected to forward Internet packets. Thus, those vehicles and IGWs are most likely to be congested. Particularly, in the case of Internet traffic burst or high vehicle density, severe medium collisions and queue overflow will happen at the congested hot-spots. Packets will be dropped accordingly, leading to a high packet loss rate. Thirdly, routing is coupled with IGW selection and vehicle mobility management. IGWs play as the destinations for the uplink Internet traffic. The dynamic routing needs to determine not only a next-hop relay but also an IGW for the Internet traffic. In addition, the reverse of the uplink forwarding path can not find the source request vehicle (SRV) in the downlink due to the fast moving of vehicles. Mobility management should be used to identify the SRV in the downlink routing.

The traditional routing protocols originally developed for mobile ad hoc networks (MANETs), such as ad hoc on-demand distance (AODV) [13], dynamic source routing (DSR) [14], destination-sequenced distance-vector (DSDV) [15], etc., need

Manuscript received March 9, 2020; revised July 11, 2020 and October 16, 2020; accepted November 16, 2020. Date of publication December 2, 2020; date of current version January 22, 2021. This work was supported in part by the National Natural Science Foundation of China under Grants U1801261, U1701265, 61 671 208, 61 971 198, and 61 671 213, in part by the Key Program of Marine Economy Development (Six Marine Industries) Special Foundation of Department of Natural Resources of Guangdong Province under Grant GDNRC [2020]009, in part by the Guangdong Basic, and in part by the Applied Basic Research Foundation under Grant 2019A1515011040, and in part by the National Key Research and Development under Project 2020YFC2005700. The review of this article was coordinated by Dr. Tao Dusit Niyato. *(Corresponding author: Quansheng Guan.)*

Ruiyan Han, Quansheng Guan, Jinglun Shi, and Fei Ji are with the School of Electronic and Information Engineering, South China University of Technology, Guangzhou 510 640, China and also with the Key Laboratory of Marine Environmental Survey Technology, and Application, Ministry of Natural Resources, Guangzhou 5 100 000, China (e-mail: ruiyanh@163.com; qshguan@gmail.com; shijl@scut.edu.cn; eefeiji@scut.edu.cn).

F. Richard Yu is with the Department of Systems and Computer Engineering, Carleton University, Ottawa, Ontario K1S 5B6, Canada (e-mail: richard.yu@carleton.ca).

Digital Object Identifier 10.1109/TVT.2020.3041948

to establish a forwarding path before data transmissions. Rerouting process is frequently triggered when the communication links are intermittently disconnected due to the mobility of vehicles. In this case, traditional routing protocols become ineffective in IoV. Existing works often used vehicles' positions to extend the routing protocols for MANETs to VANETs [16]–[20]. Queue length is a critical indicator for congestion, and has been used in routing to avoid hot-spots [21]–[23]. Particularly, the back-pressure (BP) routing uses the differential backlogs between neighboring nodes as the congestion gradients to achieve throughput-optimal in MANETs [24], [25]. However, the BP routing may lead to a loop trap and a large end-to-end delay, especially when the network load is light or moderate [26], [27]. Many works have been proposed to deal with gateway selection and mobility management for IoV [28]–[32]. Software defined network (SDN) architecture is also used to manage the joint dynamic routing, gateway selection and mobility management in IoV [33], [34]. However, the centralized coordination will introduce a large amount of signaling traffic between vehicles/gateways and the SDN controller. The centralized coordination in SDN may become the bottleneck in IoV due to the fast changing network topology [35].

Our previous work in [36] has shown that the awareness of the distance between a relay and the destination can improve the end-to-end packet delay of the BP routing for MANETs. This paper further extends our previous work to IoV. We propose a congestion and position aware per-hop routing, called distance-weighted back-pressure dynamic routing (DBDR), which is joint designed with IGW selection and mobility management to provide Internet services. The contributions of this paper are summarized as follows.

- *Distance-weighted back-pressure dynamic routing:* DBDR schedules the next hop that by prioritizing the vehicle with a large backlog differential of the buffer queues and the vehicle geographically close to the destination. Then, packets are forwarded hop-by-hop between an available IGW and a vehicle. DBDR can release the congestion at IGWs and vehicles near IGWs with the assistant of a multi-hop IGW discovery (MIGD) and a geographic location based SRV management (GLSM), and implement seamless Internet services in IoV.
- *Stability analysis for DBDR:* We prove by Lyapunov drift theory that DBDR achieves a status of network stability on the buffer queues and achieves the network capacity.

We have also carried out extensive simulations by a platform that integrates NS-2 [37] and VanetMobiSim [38] to study the proposed DBDR. Our simulations are carried out on a practical road. The simulation results show that DBDR achieves higher packet delivery ratio (PDR), end-to-end throughput, and success rate of HTTP requests/responses than the existing protocols. DBDR also achieves the lowest average packet delay (APD) when the network gets congested.

The remainder of this paper is organized as follows. Section II presents the related work, and Section III presents the system model. We propose DBDR for IoV in Section IV, and discuss its property of network stability in Section V. Simulation results are shown in Section VI. Finally, Section VII concludes this paper.

II. Related Works

This section surveys the existing works that address the challenges of dynamic topology, network congestion, and joint design with IGW discovery/selection and mobility management in IoV. To address the frequent re-routing issue of traditional routing protocols, like AODV, DSR, DSDV, etc., many works proposed to select a stable route that consists of links with the long lifetime [8], [10], [11], [39], [40]. Clustering was also considered as an alternative technique to improve routing scalability and reliability in VANETs [41]. Non-topology based dynamic routing without establishing a fixed path for data delivery is an efficient approach to deal with the dynamic topology changes. The positions of vehicles were often exploited in the existing routing protocols for VANETs [16]. The trajectory of vehicles was also used to improve data delivery [17]. The geographical positions were introduced to opportunistic routing to accurately discover the forwarding opportunities of vehicles [18], [19], [42]. It has been shown in [12] that the position-based routing is more suitable for VANETs.

To enable a bi-directional Internet access by these routing protocols, the IoV routing required to find an available IGWs for the uplink forwarding [43] and to provide mobility management for the seamless roaming and service continuity when vehicles traverse different access networks [28]. Therefore, IGW discovery/selection has been considered as an extension of the routing for connecting VANETs to the Internet. The works in [7], [9] used greedy forwarding (GF) [20] to select the relay with the greatest geographic progress towards the destination as the next-hop, combining proactive gateway discovery mechanism for Internet access. Although the GF can reduce the number of hops, vehicles who are close to IGWs may be selected as the next-hop forwarder by many vehicles and become hot-spots. Packets may lose due to queue overflow, and network throughput may degrade significantly.

Therefore, queue length is a critical congestion indicator in selecting the next-hop relay to avoid hot-spots at IGWs and vehicles near IGWs. Modeling each relay vehicle as a queueing system in [21]–[23] to control network congestion originates from the idea of the BP routing. The BP routing was first proposed in [24]. It was later extended to MANETs in [25], and then was applied in VANETs to achieve network stability and maximize network throughput. The work in [44] proposed a distributed back-pressure control approach to maximize the social welfare for a vehicular participatory sensing system. The reference [45] used the stability scheduling method based on back-pressure vector to ensure the stable state of the communication process in vehicular networks. The reference [46] proposed a multi-commodity flow back-pressure route to improve the traffic efficiency of official vehicles in VANETs. An event-aware back-pressure scheme was proposed to forward emergency packets in the shortest path and avoid the network congestion according to the queue backlog difference in IoT [27]. However, the BP routing may trap into forwarding loops [26], [27]. In this sense, the distance weighted back-pressure in our proposed DBDR makes BP destination-aware and is important to avoid loop trap.

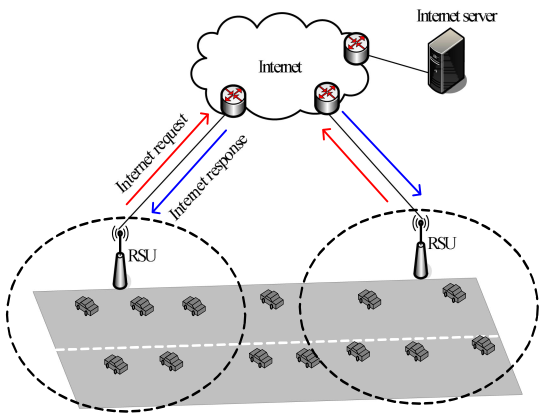

Fig. 1. Network Architecture of the IoV.

IoV also requires a position-based [31] and multi-hop based [32] mobile IP (MIP) management for downlink to provide seamless Internet access. The reference [31] proposed to partition the road into routing areas to apply MIP. The reference [32] extended MIPv6 to VANETs. The reference [47] proposed to manage vehicle mobility based on street layout as well as the distance between vehicles and base stations to integrate VANETs and fixed IP networks. The reference [48] proposed an efficient proxy mobile IPv6-based handoff scheme to provide transparent mobility support. IGW discovery and mobility management provide only information of IGWs and moving SRVs, which needs to be further integrated in routing to provide bi-directional Internet services. The design of DBDR has jointly considered the routing, IGW selection and mobility management.

III. System Model

In this section, we present the network architecture and system model for vehicular Internet access.

A. Network Architecture

This paper considers an IoV that integrates the VANET and the Internet. An IoV consists of moving vehicles randomly deployed on urban streets, and fixed RSUs at the roadside, as shown in Fig. 1. Considering that positioning is widely available in future intelligent vehicles, we assume that vehicles can obtain their own positions, e.g., using global positioning systems (GPSs). To form a VANET, we assume that vehicles and RSUs can establish link connections wirelessly with each other, e.g., using IEEE 802.11OCB (formerly known as IEEE 802.11p) [49]. The moving vehicles form a VANET, which is an autonomous system (AS) in the Internet. RSUs serve as IGWs or access points, which can connect the VANET to the IP-based Internet with the wired network. The system supports multi-hop communications to connect vehicles and RSUs.

To access the Internet, IoV should support bi-directional connections between vehicles and the Internet, including the uplink and the downlink connections. For the uplink, vehicles have to first connect to an IGW via the VANET, and the IGW will then connect to the Internet. The multi-hop forwarding within the AS of the VANET requires a dedicated routing protocol internally, which will be studied in this paper. IGWs will use the exterior gateway protocols to deliver packets from one AS to another in the Internet, which is out of scope of this paper.

For the downlink, the Internet access uses MIP to support mobility management for mobile vehicles. In the MIP environment, RSUs act as the mobility agent, Home Agents (HAs) and Foreign Agents (FAs) for vehicles. Each vehicle is configured with a unique IP address associated with its home network. The moving vehicles must register a care-of-address (CoA) with its HAs, and change its attached RSUs when moving along the road. The IP datagram from the Internet server to one SRV will be tunnelled from its HA to its current FA using its registered CoA, and then be decapsulated by its FA and forwarded to the SRV via the VANET.

B. Network Model

The network consists of N vehicle nodes and I IGW nodes. Let $\mathbf{N} = \{1, 2, \ldots, N\}$ and $\mathbf{I} = \{1, 2, \ldots, I\}$. We denote a communication link for direct transmissions from node a to node b by (a, b). We divide the time horizon into slots, denoting by $t \in \{1, 2, 3, \cdots\}$. Let $\boldsymbol{\mu}(t) = (\mu_{ab}(t))$ represent the matrix of transmission rates offered over each link (a, b) in the network during slot t. We have $\mu_{ab}(t) = 0$ when the physical link (a, b) does not exist in the network. These transmission rates must be selected within a set of possible time-varying options.

Since the network has node mobility and time-varying channels, the set of transmission rate options is described as a general function of the topology state $S(t)$. A link-rate matrix $\boldsymbol{\mu}(t)$ is admissible if the link-rates specified by $\boldsymbol{\mu}(t)$ can be achieved simultaneously. For example, in the interference range of a node, only one link can be activated, and the others should be silent. Furthermore, we assume that there exists a $\mu_{\max}$ such that $\mu_{ab}(t) \leq \mu_{\max}$, $\forall (a, b) \in L$ and for all admissible $\boldsymbol{\mu}(t)$. The shared wireless medium also leads to $\sum_b \mu_{ab}(t) \leq \mu_{max}$ and $\sum_a \mu_{ab}(t) \leq \mu_{max}$.

We use a superscript c to denote a class of packets with the same destination node c, where $c \in \mathbf{N}$ in the downlink and $c \in \mathbf{I}$ in the uplink. Define $\mu_{ab}^{(c)}(t)$ as the routing variable representing the data rate for packets c delivered over link (a, b) during slot t, subject to the following constraints:

$$\sum_{c \in \mathbf{N} \cup \mathbf{I}} \mu_{ab}^{(c)}(t) \leq \mu_{ab}(t), \tag{1}$$

$$\mu_{ab}^{(c)}(t) = 0, \text{ if } (a, b) \notin L_c, \tag{2}$$

where L_c is defined as the set of all links allowed to transmit packets c. The constraint in (1) means that the sum rate for packets delivered over link (a, b) is not larger than the transmission rate of the link.

C. Queueing Model

To facilitate the decision on the routing variables $\mu_{ab}^{(c)}(t)$, we classify packets in the network by their destinations. The buffer in a node is divided into different queues, and each queue is used to buffer packets for a destination. Thus, the arriving packets will be enqueued into separate queues according to their destinations. Define $\{i, c\}$ as the queue c in node i and $D_i^{(c)}$ as the Euclidean distance between node i and the corresponding

TABLE I
MAIN USED SYMBOLS IN OUR PAPER

Symbols	Description
$\mu_{ab}(t)$	The transmission rate offered over each link $(a,\ b)$ during slot t.
$D_i^{(c)}$	The Euclidean distance between node i and the corresponding destination node c.
$U_i^{(c)}(t)$	The amount of undelivered packets c at node i.
$WQ_{ab}^{(c)}(t)$	The distance-weighted backlog differential of packets c over a link $(a,\ b)$.
$A_i^{(c)}(t)$	The process of exogenous packets arriving at the source node i and destinating for c.
$\lambda_i^{(c)}$	The average arrival rate of the packets that are destined for node c at node i.

destination node c. We assume that $D_i^{(c)}(t) \leq D_{\max}$. Let $U_i^{(c)}(t)$ denote the amount of undelivered packets c at node i. Particularly, $U_i^{(c)}(t) = 0$ if $i = c$, since packets at the destination node will be delivered to the transport layer directly, thus queue $\{i, i\}$ does not exist. Nevertheless, we assume that this queue $\{i, i\}$ exists and its packet backlogs $U_i^{(i)}(t) = 0$ for convenience of analysis. Thus, each node maintains at most N queues for the downlink and I queues for the uplink.

The main notations used in the discussion are list in Table I.

IV. Dynamic Routing for Vehicular Internet Access

This section presents our proposed dynamic routing for vehicular Internet access, which is jointly designed with IGW selection and vehicle mobility management.

A. Distance-Weighted Back-Pressure Dynamic Routing

Our proposed DBDR provides multi-hop forwarding service for IP datagrams between an SRV and an IGW, supporting both uplink and downlink forwarding. DBDR consists of three steps, including queue scheduling, link scheduling, and routing decision, which will be elaborated next.

1) Queue Scheduling: In our queueing model, the packets destined for different destinations have been enqueued into separate queues. Once a queue is scheduled, its head-of-line packet will be dequeued to send. In this sense, scheduling a queue is equivalent to selecting a destination.

The traditional BP algorithm uses the backlog differentials as a congestion gradient to schedule multiple queues, i.e.,

$$c_{ab}^{opt}(t) = \arg \max_{\{c,(a,b)\in L_c\}} [U_a^{(c)}(t) - U_b^{(c)}(t)], \tag{3}$$

which means that the queue c in link (a, b) has the largest backlog differential, and head-of-line of the queue c will be dequeued to send. Suppose that node a is congested, and node b is idle (i.e., its buffer is empty.). The next-hop selection strategy in (3) can quickly release the congestion in node a, and will not make node b congested. Take the queue backlogs as the fluid pressure. Since the destination node is the sink of data transmissions, its queue backlog is always empty. The principle behind (3) just likes "water flows from high pressure to low pressure". As long as there are backlogs in the network, the backlog data packets will be delivered to the destination sooner or later.

The scheduling in (3) considers only the backlog differentials between neighboring nodes, and is not aware of the positions of destinations. Forwarding loop trap or unnecessary long forwarding paths may exist in the network, because no sufficient pressure gradients are built up towards its destination particularly when the traffic loads are light. Thus, scheduling based on only backlog differentials have been known to lead to a long end-to-end delivery delay.

In DBDR, we use a distance-weighted backlog differential to schedule queues, which is defined as follow,

$$WQ_{ab}^{(c)}(t) = w_1 U_a^{(c)}(t) - w_2 \frac{D_b^{(c)}(t)}{D_a^{(c)}(t)} U_b^{(c)}(t), \tag{4}$$

where $w_1 + w_2 = 1$, $w_1, w_2 \in (0, 1)$; $D_b^{(c)}(t)$ denotes the distance between the next-hop candidate node b and the destination c at time t; $D_a^{(c)}(t)$ denotes the distance between the sender node a and the destination c at time t. When node b is close to destination c, the distance ratio in (4) will be large, leading to a large $WQ_{ab}^{(c)}$. However, the backlog differential in (3) cannot distinguish the next-hop relays that have different distances from the destination.

The queue having the maximum weighted backlog differential is then scheduled for forwarding, i.e.,

$$c_{ab}^{opt}(t) = \arg \max_{\{c,(a,b)\in L_c\}} WQ_{ab}^{(c)}(t). \tag{5}$$

We use the distance ratio of $\frac{D_b^{(c)}(t)}{D_a^{(c)}(t)}$ to weigh the backlog of a relay candidate. Thus, the distance weights play a role of geographical distance gradients toward destinations. In this way, even without enough congestion gradients, the packets can still be forwarded to the destination. The coefficients w_1 and w_2 can be further used to adjust the weights on the distance-weighted backlogs, and provide tradeoff between congestion avoidance and the geographically greedy forwarding.

We then define the weighted backlog differential for a link (a, b) as follow,

$$WQ_{ab}(t) = \max\left(WQ_{ab}^{(c_{ab}^{opt}(t))}(t), 0\right). \tag{6}$$

The calculations of (5) are different for uplink and downlink forwarding, due to the different destinations.

- *Uplink:* The destination of uplink forwarding is an IGW in IoV. Due to the multi-hop nature of the MIGD mechanism, several IGWs might be available when one vehicle locates within the overlapping service area of multiple gateways. In this case, the vehicle has to decide which IGW currently as its destination to avoid congestion and reduce delay. Thus, we should have $c \in \mathbf{I}$ in (5) to select the best IGW.
- *Downlink:* The responses from the Internet server will be returned back to the HA in the home network. In this case, since SRVs become the destination nodes, we should have $c \in \mathbf{N}$ in (5). Then, the Internet packets will be delivered to SRVs by HAs/FAs in the downlink direction.

2) Link Scheduling: DBDR schedules transmission links and chooses the next forwarder to maximize a weighted throughput using the weighted backlog differential $WQ_{ab}(t)$ as the weight, i.e., DBDR determines the transmissions rates $\boldsymbol{\mu}(t)$ for links using the following criterion:

$$\underset{\boldsymbol{\mu}(t)}{\text{maximize}} \quad \sum_{ab} WQ_{ab}(t)\mu_{ab}(t), \tag{7}$$

$$\text{subject to} \quad \boldsymbol{\mu}(t) \in \Gamma_{S(t)}, \tag{8}$$

where $\Gamma_{S(t)}$ is the set of rate space. We can see from (4) and (6) that a larger backlog differential will lead to a larger $WQ_{ab}(t)$; a relay that is closer to the destination will also lead to a larger $WQ_{ab}(t)$. Using (7), the link with a high weight and high capacity will be scheduled to be active, and other links in its interference range will be silent.

According to (7), DBDR will schedule the link with prioritization of the closest relay and the largest backlog differential. Since the nodes near the destination have a high probability to be congested, the backlogs in their queues will be large. However, these nodes also have small distance ratio. According to (4), these nodes will have small distance-weighted backlog differentials. They will not be scheduled as the next-hop relay by (7) to release their congestion.

On the other hand, the introduction of distance ratio in (4) will make the forwarding by DBDR progressively towards the nodes that are close to the destination. In this way, DBDR can avoid loop trap which may happen in BP.

3) Routing Decision: Finally, DBDR allocates a transmission rate of $\mu_{ab}^{(c)}(t)$ to the scheduled link and scheduled queue. Denote the allocated transmission rates under DBDR by $(\mu_{ab}^{*(c)}(t))$, and the solution for the optimization problem (7) by $\mu_{ab}^{opt}(t)$. Then, DBDR offers the available rate of $\mu_{ab}^{opt}(t)$ to the scheduled queue, i.e.,

- $\mu_{ab}^{*(c)}(t) = \mu_{ab}^{opt}(t)$, if $c = c_{ab}^{opt}(t)$, where $c_{ab}^{opt}(t)$ is the scheduled queue by (5);
- $\mu_{ab}^{*(c)}(t) = 0$, otherwise.

In addition, DBDR adopts store-carry-forward mechanism when no reachable neighbor is available. To prevent packets from being carried all the time, we set up a carry timer for the scheduled packet. The packet is forwarded and removed from the cache once a suitable next-hop can be found before its carry timer expires. Otherwise, the packet is discarded.

DBDR only needs to determine the next-hop forwarding based on the neighboring information, e.g., queue backlogs and neighbor positions. The signaling traffic is reduced significantly, comparing to the traditional routing protocols (such as AODV, DSDV, DSR), which have to search for and maintain the multi-hop forwarding path for data transmissions in the frequently changing VANET.

B. Implementation of DBDR in Vehicle Networks

The implementation of DBDR in vehicle networks requires discovery of available IGWs, locations and queue backlogs of neighbors and IGWs, and mobility management of moving SRVs.

1) Multi-Hop IGW Discovery (MIGD): We use the agent advertisements (AAMs) in MIP to advertise the existence of IGWs, which provide Internet access services. To enable the multi-hop forwarding for Internet access in VANETs, we need to extend the service range of an IGW. However, the traditional MIP always sets the IP time-to-live (TTL) field to one in AAMs, which limits the service range of an IGW to one hop [50]. Due to the scarce deployment of IGWs, our proposed MIGD sets the TTL to a value that is larger than 1 to extend the broadcast range of AAMs. To facilitate the design of the multi-hop routing in Section IV-A, we also allow the AAM to carry the IGW's position information.

Algorithm 1: Processing Algorithm at a Vehicle on Receiving an AAM.

```
if TTL > 0 then
  TTL ← TTL − 1
  if There exists an entry then
    if SeqNum in the AAM > SeqNum in the buffer then
      Update the received AAM
      Rebroadcast the updated AAM to all neighbors
    else
      Discard the AAM
    end if
  end if
  if There does not exist an entry then
    Create a new IGW entry in the IGW list
    Rebroadcast the AAM to all neighbors
  end if
else
  Discard the AAM
end if
```

To avoid broadcast storm and bandwidth waste, the sequence number (SeqNum) field in AAMs is adopted to limit redundant rebroadcasts of AAMs. The SeqNum is incremented by one once a new AAM is generated, and the vehicle only rebroadcasts the AAM that has a greater SeqNum than its known maximum one.

Each vehicle maintains an IGW list, where each entry in the list has a period of validity. On receiving an AAM, the vehicle will verify the validity of the AAM by checking its TTL, and will then rebroadcast the AAM to its neighbors or drop the AAM. The detailed processing for AAM is summarized in Alg. 1.

2) Exchanges of Neighboring Locations and Backlogs: DBDR needs the neighboring locations and backlogs to compute the weighted backlog differentials, as shown in (4). Each vehicle uses a periodic beacon mechanism to broadcast its geographic location and queue backlogs.

Each vehicle can then establish a neighbor table in the buffer using the exchanged information from one-hop neighbors. An entry for the neighbor table includes node IP address, geographic location, queue backlogs. Each neighbor entry in a vehicle has a period of validity. However, it is inevitable that some neighbors will move out of the vehicle's communication range within the validity period. In this case, DBDR may use outdated neighbors, leading to forwarding failures. The routing layer only relies on the beacon mechanism to detect the invalid neighbors. On the other hand, the MAC layer considers a neighbor unreachable when the frame transmissions to that neighbor fail for several times. Therefore, we allow the MAC layer to feed back the link failures to the routing layer, and then will be deleted the corresponding entry from the neighbor table. This helps the routing layer discover invalid neighbors in time without waiting for the expiration of the neighbor entry, thus reducing packet losses. Since DBDR does not rely on path computation, deleting a neighbor entry does not affect the end-to-end forwarding. Any changes of a neighbor entry will trigger the reconfiguration by the algorithm described in Section IV-A.

It is noticed that DBDR does not need to obtain the global network topology, or find and maintain an end-to-end forwarding path before data transmissions, due to its dynamic forwarding feature. In this sense, DBDR has much lower signaling traffic than the existing traditional routing protocols like AODV, DSDV, DSR, etc.

3) Geographic Location Based SRV Management (GLSM): DBDR needs the exact location of the SRV to deliver the response packets from the Internet server in the downlink forwarding. However, the SRV may have changed its location and moved to the service coverage of another IGW. The existing MIP only determines which IGW the SRV is currently in, but cannot determine the position of the SRV. It is also difficult for IGWs to request the SRVs' locations on demand due to the high mobility of SRVs.

We allow vehicles register their locations spontaneously to their associated IGWs. The IGW acts as the local location management agent for the vehicles within its multi-hop service range. The HA/FA receives the registration and then establishes a visit list to record the location of the vehicle. The Internet responses from the Internet server would be sent to the HA of the SRV. The HA detects whether the SRV stays in the home network using CoA. If the SRV locates in the foreign network, the response packets are tunneled to the corresponding FA and decapsulated by the FA. Finally, the HA/FA obtains the position information of the SRV from the location management agent, and the packets can be sent to the corresponding SRV using our proposed DBDR algorithm.

V. Network Stability Analysis

In this section, we will show how DBDR can ensure the network stability by using *Lyapunov drift*.

A. Network Stability

Let $A_i^{(c)}(t)$ with $i, c \in \mathbb{N}$ represent the process of exogenous packets arriving at the source node i and destinating for c. Assume that $A_i^{(c)}(t)$ follows an independent and identical distribution $(i.i.d)$ and $A_i^{(c)}(t) \leq A_{\max}$ for all i, c and t. Let $A_i(t) = \sum_{c \in \mathbf{N} \cup \mathbf{I}} A_i^{(c)}(t)$.

All exogenous arrivals directly enter the network layer at their source nodes. The queueing dynamics thus satisfy:

$$U_i^{(c)}(t+1) \leq \max\left[U_i^{(c)}(t) - \sum_b \mu_{ib}^{(c)}(t), 0\right] + A_i^{(c)}(t) + \sum_a \mu_{ai}^{(c)}(t), \tag{9}$$

where $\sum_b \mu_{ib}^{(c)}(t)$ is the sending packets, and $\sum_a \mu_{ai}^{(c)}(t)$ is relayed packets from neighbors. The network stability is defined on the queue backlogs $U_i^{(c)}(t)$ as follow.

Definition 1 (Network stability): The network is strongly stable, if all queues of nodes in the network are strongly stable, satisfying the following condition,

$$\lim_{t\to\infty} \sup_i \frac{1}{t} \sum_c \mathbb{E}\left\{U_i^{(c)}(t)\right\} < \infty. \tag{10}$$

Let $\mathbb{E}[A_i^{(c)}(t)] = \lambda_i^{(c)}$. We can define $\boldsymbol{\lambda} = (\lambda_i^{(c)})$ as the matrix of arrival rates and $\boldsymbol{\Lambda}$ as the capacity region. Then the network stability satisfies the following conditions: (a) a necessary condition is $\boldsymbol{\lambda} \in \boldsymbol{\Lambda}$; (b) a sufficient condition is that $\boldsymbol{\lambda}$ is strictly interior to $\boldsymbol{\Lambda}$, i.e., $\boldsymbol{\lambda} + \boldsymbol{\epsilon} \in \boldsymbol{\Lambda}$ for some $\varepsilon > 0$[25].

B. Analysis of Network Stability

According to the definition of network stability, it requires the expectation of the queue backlog to be bounded. We next prove the network stability of DBDR by Lyapunov drift theory. We first define Lyapunov function as:

$$L[\boldsymbol{U}] = \sum_{i,c \in \mathbf{N} \cup \mathbf{I}} w_i D_i^{(c)} \left(U_i^{(c)}\right)^2, \tag{11}$$

where $w_i \in \{w_1, w_2\}$ is the weight on the distance-weighted backlogs as (4).

The following lemma [51] is useful in our analysis.

Lemma 1: If V, U, μ, A are nonnegative real numbers and

$$V \leq \max[U - \mu, 0] + A, \tag{12}$$

then

$$V^2 \leq U^2 + \mu^2 + A^2 - 2U(\mu - A). \tag{13}$$

Combining Lemma 1 with inequality (9), we can obtain the following inequality:

$$\left(U_i^{(c)}(t+1)\right)^2 \leq \left(U_i^{(c)}(t)\right)^2 + \left(\sum_b \mu_{ib}^{(c)}(t)\right)^2 + \left(A_i^{(c)}(t) + \sum_a \mu_{ai}^{(c)}(t)\right)^2 - 2U_i^{(c)}(t)\left[\sum_b \mu_{ib}^{(c)}(t) - A_i^{(c)}(t) - \sum_a \mu_{ai}^{(c)}(t)\right].$$

Since we have assumed $\sum_b \mu_{ib}^{(c)}(t) \leq \mu_{max}$, $\sum_a \mu_{ai}^{(c)}(t) \leq \mu_{max}$, and $A_i^{(c)}(t) \leq A_{max}$, the above inequality can be transformed into

$$\left(U_i^{(c)}(t+1)\right)^2 \leq \left(U_i^{(c)}(t)\right)^2 + \mu_{max}^2 + (A_{max} + \mu_{max})^2 - 2U_i^{(c)}(t)\left[\sum_b \mu_{ib}^{(c)}(t) - \sum_a \mu_{ai}^{(c)}(t) - A_i^{(c)}(t)\right].$$

Multiplying the two sides of the above inequality by $w_i D_i^{(c)}$ and then summing over all entries (i, c), we obtain the following

Lyapunov drift,

$$\begin{aligned}\triangle L &= L[\boldsymbol{U}(t+1)] - L[\boldsymbol{U}(t)] \\ &\leq M + 2\sum_{ic} w_i D_i^{(c)} U_i^{(c)}(t) A_i^{(c)}(t) \\ &\quad - 2\sum_{ic} w_i D_i^{(c)} U_i^{(c)}(t) \left[\sum_b \mu_{ib}^{(c)}(t) - \sum_a \mu_{ai}^{(c)}(t)\right],\end{aligned}$$

where

$$M \triangleq w_{max} D_{max} \sum_{i,c\in\mathcal{N}} \left[\mu_{max}^2 + (A_{max} + \mu_{max})^2\right],$$

and $w_{max} = \max(w_1, w_2)$. Then, the conditional Lyapunov drift becomes

$$\begin{aligned}&\mathbb{E}[\triangle L \,|\, \boldsymbol{U}(t)] \leq M + 2\sum_{ic} U_i^{(c)}(t) E\left\{w_i D_i^{(c)} A_i^{(c)}(t) \,|\, U(t)\right\} \\ &-2\mathbb{E}\left\{\sum_{ic} w_i D_i^{(c)} U_i^{(c)}(t)\left[\sum_b \mu_{ib}^{(c)}(t) - \sum_a \mu_{ai}^{(c)}(t)\right] | U(t)\right\}.\end{aligned} \tag{14}$$

Since the arrival $A(t)$ is *i.i.d.* over time slots, we have

$$\begin{aligned}\mathbb{E}\{w_i D_i^{(c)} A_i^{(c)}(t) \,|\, U(t)\} &\leq w_{max} D_{max} \mathbb{E}\{A_i^{(c)}(t) \,|\, U(t)\} \\ &= w_{max} D_{max} \lambda_i^{(c)}.\end{aligned} \tag{15}$$

By the following transformation, we have

$$\begin{aligned}&\sum_{ic} w_i D_i^{(c)} U_i^{(c)}(t) \left[\sum_b \mu_{ib}^{(c)}(t) - \sum_a \mu_{ai}^{(c)}(t)\right] \\ &= \sum_{icb} w_i D_i^{(c)} U_i^{(c)}(t) \mu_{ib}^{(c)}(t) - \sum_{ica} w_i D_i^{(c)} U_i^{(c)}(t) \mu_{ai}^{(c)}(t) \\ &= \sum_{acb} w_1 D_a^{(c)} U_a^{(c)}(t) \mu_{ab}^{(c)}(t) - \sum_{bca} w_2 D_b^{(c)} U_b^{(c)}(t) \mu_{ab}^{(c)}(t) \\ &= \sum_{ab}\sum_c \mu_{ab}^{(c)}(t) \left[w_1 D_a^{(c)} U_a^{(c)}(t) - w_2 D_b^{(c)} U_b^{(c)}(t)\right].\end{aligned} \tag{16}$$

According to (4) and (7), we have

$$\begin{aligned}&\sum_{abc} \mu_{ab}^{(c)}(t) \left[w_1 D_a^{(c)} U_a^{(c)}(t) - w_2 D_b^{(c)} U_b^{(c)}(t)\right] \\ &= \sum_{ab}\sum_c \mu_{ab}^{(c)}(t) D_a^{(c)} W Q_{ab}(t) \\ &\leq \sum_{abc} \mu_{ab}^{opt}(t) D_a^{(c)} W Q_{ab}(t) \\ &\leq \sum_{abc} \mu_{ab}^{*(c)}(t) \left[w_1 D_a^{(c)} U_a^{(c)}(t) - w_2 D_b^{(c)} U_b^{(c)}(t)\right],\end{aligned} \tag{17}$$

where the inequality (17) follows according to the routing decision strategy of DBDR in Section IV-A3. Substituting (16) into (17), we have

$$\begin{aligned}&\sum_{ic} w_i D_i^{(c)} U_i^{(c)}(t) \left[\sum_b \mu_{ib}^{(c)}(t) - \sum_a \mu_{ai}^{(c)}(t)\right] \\ &\leq \sum_{ic} w_i D_i^{(c)} U_i^{(c)}(t) \left[\sum_b \mu_{ib}^{*(c)}(t) - \sum_a \mu_{ai}^{*(c)}(t)\right].\end{aligned} \tag{18}$$

Hence, using (15) and (18), we can rewrite (14) as follow,

$$\begin{aligned}&\mathbb{E}[\triangle L \mid \boldsymbol{U}(t)] \leq M + 2w_{max} D_{max} \lambda_i^{(c)} \sum_{ic} U_i^{(c)}(t) \\ &-2\mathbb{E}\left\{\sum_{ic} w_i D_i^{(c)} U_i^{(c)}(t)\left[\sum_b \mu_{ib}^{*}(t) - \sum_a \mu_{ai}^{*}(t)\right] | U(t)\right\}.\end{aligned} \tag{19}$$

Suppose the traffic arrival rate is within network stability region, i.e., $\boldsymbol{\lambda} + \boldsymbol{\epsilon} \in \boldsymbol{\Lambda}$ [25], we have:

$$\mathbb{E}\left\{\left[\sum_b \mu_{ib}^{*(c)}(t) - \sum_a \mu_{ai}^{*(c)}(t)\right] \mid \boldsymbol{U}(t)\right\} = \lambda_i^{(c)} + \epsilon. \tag{20}$$

Substituting (20) into (19), we have

$$\mathbb{E}[\triangle L \mid \boldsymbol{U}(t)] \leq M - 2\epsilon \cdot w_{max} D_{max} \sum_{ic} U_i^{(c)}(t). \tag{21}$$

Further summing both sides of the above inequality from slot 0 to slot T ($T > 0$) and assuming that $\boldsymbol{U}(0) = 0$, we have,

$$\frac{L[\boldsymbol{U}(T)]}{T} \leq M - 2\epsilon \cdot w_{max} D_{max} \frac{\sum_{t=0}^{t=T-1} \sum_{ic} U_i^{(c)}(t)}{T}. \tag{22}$$

Since $\frac{L[\boldsymbol{U}(T)]}{T} \geq 0$, we can obtain the upper-bound for the average queue length by DBDR in the following,

$$\lim_{T\to\infty} \frac{\sum_{t=0}^{t=T-1} \sum_{ic} U_i^{(c)}(t)}{T} \leq \frac{M}{2\epsilon \cdot w_{max} D_{max}}. \tag{23}$$

The above inequality meets the requirement of network stability in Definition 1, and proves the stability of DBDR.

VI. Simulation Results

In this section, we evaluate the performance and effectiveness of our proposed dynamic routing using the integrated platform of VanetMobiSim and NS-2. VanetMobiSim is used for mobility simulation, and is responsible for defining the road topology and generating the moving track of the vehicle. The mobility model VanetMobiSim provides a vehicle movement model with lane changes, overtaking and shifting, and then generates an available movement track file for NS-2. NS-2 implements our proposed DBDR protocol.

We compare our proposed DBDR protocol with the dynamic BP routing protocol [24], DSDV [15] and GPSR [20]. BP uses the backlog differentials without distance weights (i.e., (3)) to schedule queues. DSDV and GPSR are classic routing protocols for MANETs. DSDV considers only the hop distance, while GPSR adopts distance-based greedy forwarding.

A. Simulation Environment and Settings

1) Road Model: We select the Ring Road at Guangzhou University City, China. Its corresponding road topology is shown in Fig. 2. The IGW is implemented in the RSU. The vehicles are randomly distributed in the road, and the IGWs are randomly located at the roadside. The vehicle speed in the simulations follows a uniform independently identically distribution in the interval of $[40, 70]$ km/h. The vehicles follow the Intelligent

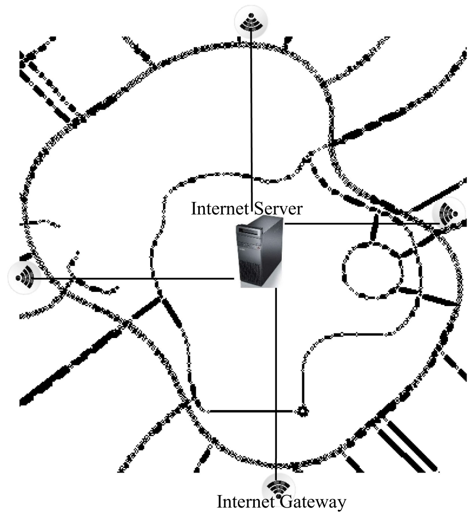

Fig. 2. Road topology of Ring Road at Guangzhou University City.

TABLE II
SIMULATION PARAMETER SETUP

Parameter	Parameter Settings
MAC type	802.11p
Wireless transmission range	250 m
Wireless data rate	2 Mbps
Interface buffer length	50 packets
TCP maximum packet length	1460 Bytes

driving model with intersection management (IDM_IM) model in VanetMobiSim [38].

The IGWs are connected to an HTTP web server via wired links, as shown in Fig. 2. The vehicles establish TCP connections with the web server to obtain Internet services.

2) Network Settings: Vehicles are equipped with IEEE 802.11p wireless interfaces [49]. The other parameters for the wireless nodes are shown in Table II.

The vehicles generate HTTP traffic by PackMimeHTTP module in NS-2. PackMimeHTTP provides several parameters to adjust the HTTP traffic, including HTTP connection rate, HTTP protocol version, etc. The HTTP connection rate refers to the number of the generated HTTP connections per second. The generation of HTTP connections follows a Poisson process with the HTTP connection rate as its intensity. Thus, the HTTP connection rate can adjust the traffic loads in the network. We enable the HTTP/1.1 option in HTTP protocol version to support persistent connections.

The beacon interval of DBDR is set to 2 seconds to update the dynamic buffer backlogs and positions. The AAM interval in MIP is set to 4 seconds. The TTL value of the AAM is set to 4, and the registration interval is set to 2 seconds. We also enable the store-carry-forward manner in the multi-hop forwarding when there is no next-hop neighbor available around. The carrying time for packets is set to 18 seconds.

3) Performance Metrics: We use the following metrics to evaluate the performance of the routing protocols in provisioning Internet services.

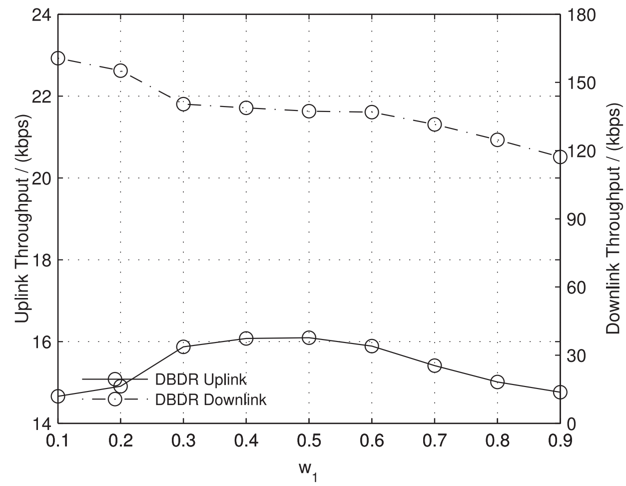

Fig. 3. Throughput of the DBDR with different w_1.

- *PDR:* The ratio of the total number of successfully received packets to the total number of sent packets, which reflects the reliability and stability of the routing.
- *APD:* The average end-to-end delivery delay for successfully received packets at the destination, including queuing delay, transmission delay and retransmission delay.
- *Throughput:* The effective amount of data transmitted in a unit time in the network.
- *Success rate of HTTP requests/responses:* We use HTTP request success rate (ReqST) and HTTP response success rate (ResST) to evaluate the uplink performance and the downlink performance for Internet services. The HTTP ReqST is the ratio of the total number of HTTP requests successfully received by the Internet server to the total number of HTTP requests sent by the SRVs. The HTTP ResST is the ratio of the total number of HTTP responses successfully received by the SRV and the total number of HTTP responses sent by the Internet server. The HTTP success rate relates to the quality of experience (QoE) for Internet users.

B. Simulation Results and Performance Evaluation

We study the impact of the weight w_1, the number of vehicles, the number of IGWs, and HTTP connection rate on routing performance.

1) Impact of w_1: DBDR uses w_1 and w_2 to weigh queue backlogs and provides tradeoff between congestion avoidance and the geographically greedy forwarding. We set the number of IGWs to 4, the number of vehicles to 90, and the HTTP connection rate to 20 connections per second to study how to set the weight parameters for DBDR. We have proven in Section V that DBDR can reach the network stability and the network capacity region, which relates to the throughput performance. Due to the space limit, we focus on the throughput of DBDR to study the impact of the weights.

The simulation result is shown in Fig. 3. For the uplink routing, IGWs serve as the destinations, and a large number of uplink Internet packets have the same destination due to the scarcity of IGWs. The distance is the main factor affecting network

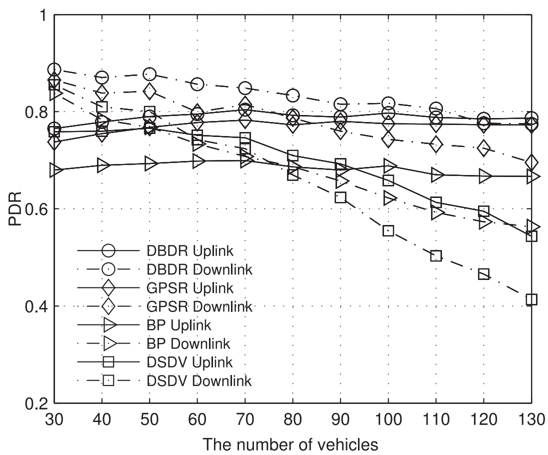

Fig. 4. PDRs of the routing protocols with different numbers of vehicles.

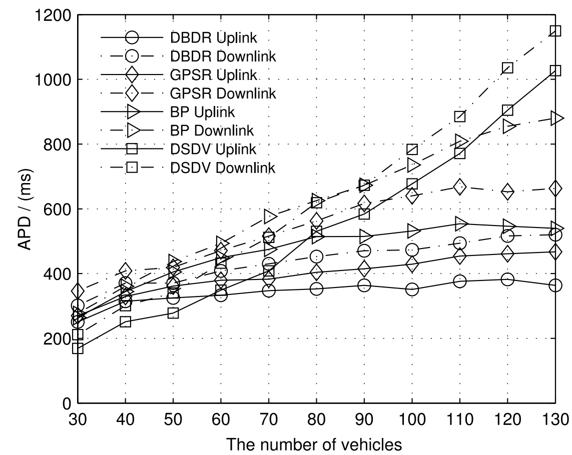

Fig. 5. APDs of the routing protocols with different numbers of vehicles.

performance when the value of w_1 is small. Vehicles close to the destination, especially vehicles near IGWs, are then likely to be selected as the next hop by multiple vehicles at the same time. Uplink Internet traffic will be aggregated at those selected vehicles, resulting in network congestion. When w_1 is getting large, the backlog becomes the main factor that determines the forwarding, which may possibly fall into a loop trap. Thus, Fig. 3 shows that the uplink throughput reaches its maximum at a w_1 between 0.3 and 0.6.

For the downlink routing, SRVs serve as the destinations, and a large number of downlink Internet packets are forwarded to different destinations. Due to the fast moving of vehicles, the positions of SRVs become the important factor that determines the downlink forwarding. Having the knowledge of SRVs positions, the downlink packets will be quickly forwarded to the corresponding destination. Therefore, the downlink throughput is decreased with w_1 due to the fast moving of SRVs as shown in Fig. 3, which can achieve a good tradeoff between greedy forwarding and congestion avoidance.

Based on the result in Fig. 3, we set $w_1 = 0.3$ and $w_2 = 0.7$ in the following simulations.

2) Impact of the Number of Vehicles: As the number of vehicles in the network increases, the Internet traffic loads will increase. To study the impact of different vehicle numbers on routing performance, we set the number of IGWs to 4 and the HTTP connection rate to 20 connections per second.

Fig. 4 shows that the PDRs with different number of vehicles. The uplink and downlink PDRs of DBDR are always higher than those of BP, DSDV and GPSR. As the number of vehicles increases, the PDRs of BP, DSDV and GPSR decrease more quickly than that of DBDR. Particularly in the uplink forwarding, the backlog-based BP routing achieves a higher PDR than the distance-based DSDV routing when the number of vehicles is larger than 90, although the PDR of BP is lower than that of DSDV when the number of vehicles is less than 90. This is because that DSDV will introduce more control messages to DSDV when the number of vehicles increases. The network will then get increasingly congested. Our proposed DBDR uses the distance-weighted backlogs in making the routing decisions. It can avoid the loop trap in the lightly congested network and release quickly the congested links in the heavily congested network.

When the number of vehicles in the network get larger, the number of packet drops due to unavailable next hop becomes smaller. The main reason for the packet drops in this case becomes the buffer overflow. From Fig. 4, we can see that the advantage of DBDR over GPSR increases when the number of vehicles increases. This is because GPSR uses only the distance in forwarding, neglecting the congestion issue at vehicles near the IGW. The distance-weighted back-pressure has avoided the hot-spots near IGWs to achieve a higher PDR.

It is shown in Fig. 5 that the APDs of the four protocols increase as the number of vehicles increases. The shortest path DSDV routing achieves the lowest APD when the network is lightly congested, e.g., there are less than 60 vehicles in the network as shown in Fig. 5. However, the APD of DSDV will increase more quickly than that of DBDR as the network gets increasingly congested, and DBDR achieves the lowest APD when the number of vehicles becomes larger than 60. Together with the results in Fig. 4, we can also conclude that DSDV achieves a lower APD by dropping more packets when no available path is available on packet arrivals, comparing to DBDR.

DBDR achieves the highest throughput as shown in Fig. 6. As the number of vehicles increases, the downlink throughput of DSDV decreases significantly, due to the negligence of congestion consideration in DSDV. The downlink throughput is always higher than the uplink throughput, since the HTTP response traffic is usually much higher than the request traffic.

Fig. 7 shows the success rate of HTTP requests/responses from the application layer. DBDR achieves the highest HTTP success rate in different numbers of vehicles. The changes of the HTTP success rate curves are similar to the PDR curves in Fig. 4, although they are not exactly the same. This is because HTTP applications are attached to TCP connections, which will retransmit lost HTTP packets. The ReqST corresponds to the uplink PDR, and the ResST corresponds to the downlink PDR.

3) Impact of the Number of IGWs: We set the number of vehicles to 90 and the HTTP connection rate to 20 connections per second to study the impact of the IGWs on routing performance.

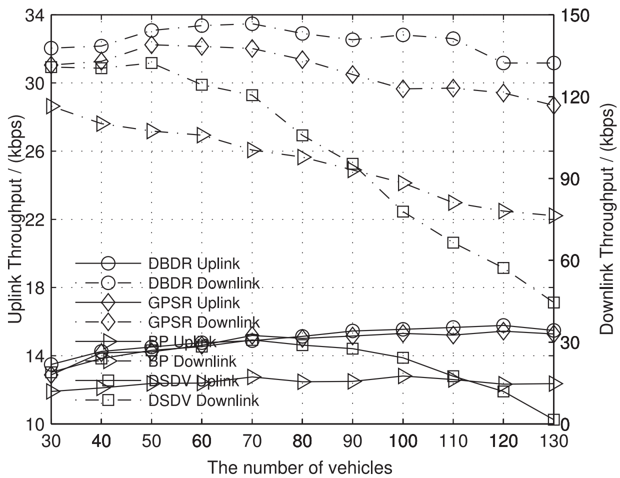

Fig. 6. Throughput of the routing protocols with different numbers of vehicles.

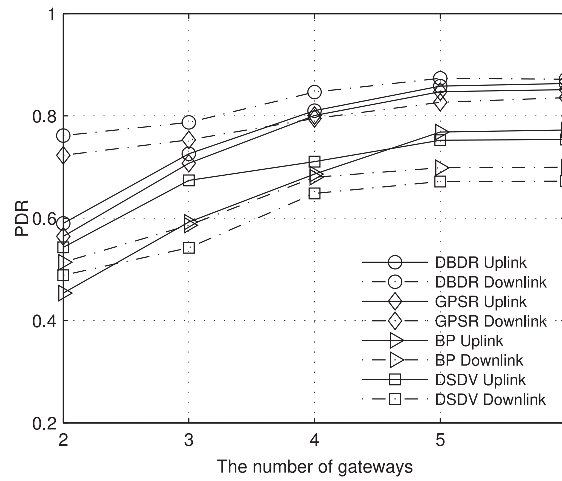

Fig. 8. PDRs of the routing protocols with different numbers of IGWs.

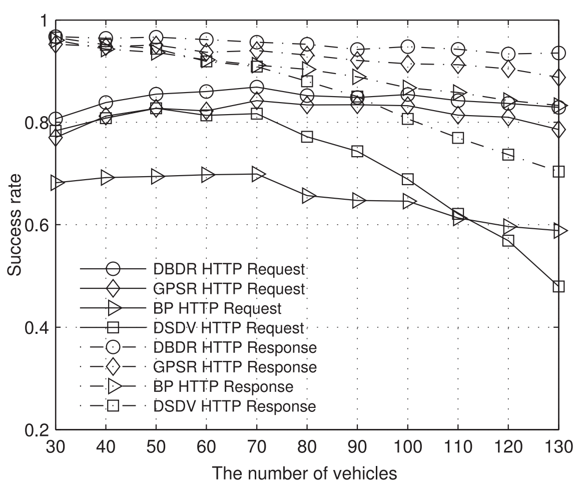

Fig. 7. HTTP request and response success rates of the routing protocols with different numbers of vehicles.

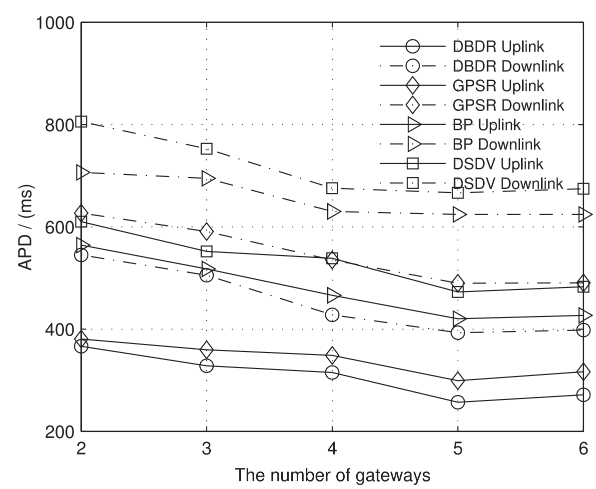

Fig. 9. APDs of the routing protocols with different numbers of IGWs.

Fig. 8 shows that the PDRs with different numbers of IGWs. As shown in the figure, when the number of IGWs in the network is small, the network lacks sufficient gateway coverage, leading to packet losses and a low PDR. As the number of IGWs increases, PDRs of all the four routing protocols increase due to the coverage improvement. DBDR always achieves the highest uplink and downlink PDRs among the four routing protocols, and consequently achieves the highest HTTP success rates as observed in Fig. 11.

When the number of IGWs is small, the IGWs cannot cover all the vehicles in the network, and a vehicle may not have an available next hop to maintain the Internet connectivity. In this case, the vehicle has to store-carry-forward its Internet packets, resulting in a higher APD. As shown in Fig. 9, The APDs of all the four routing protocols decrease with the increase of the number of the IGWs, since the increasing of the IGW number also improves the network coverage. However, DBDR can still achieve the lowest APD.

As shown in Fig. 10, it is no doubt that DBDR achieves the highest throughput with the highest PDR and the lowest APD. The throughput of the four protocols increases with the IGW number, and then maintains stable to meet the fixed traffic demand in the simulation.

From Figs. 8–11, we can see that the performance metrics, including PDR, throughput, and HTTP success rate, increase when the number of gateways increases from 2 to 5. However, the performance remains relatively stable when the number of gateways exceeds 5. The increasing of the number of gateways cannot continuously improve the network performance. More gateways may bring a higher cost for network deployment. In this sense, there exists an optimal number of gateways in the network, e.g., the optimal number is 5 in our simulations.

4) Impact of the HTTP Connection Rate: The HTTP connection rate also determines traffic loads in the network given a fixed number of vehicles. We set the number of vehicle to 90 and the number of IGWs to 4 to study the impact of different HTTP connection rates on routing performance.

The PDRs of all the four routing protocols decrease with the increase of the HTTP connection rate, and DBDR always achieves a higher PDR than the other three protocols, as shown in Fig. 12. Since the network capacity is limited, increasing the HTTP connection rate will introduce more traffic loads to

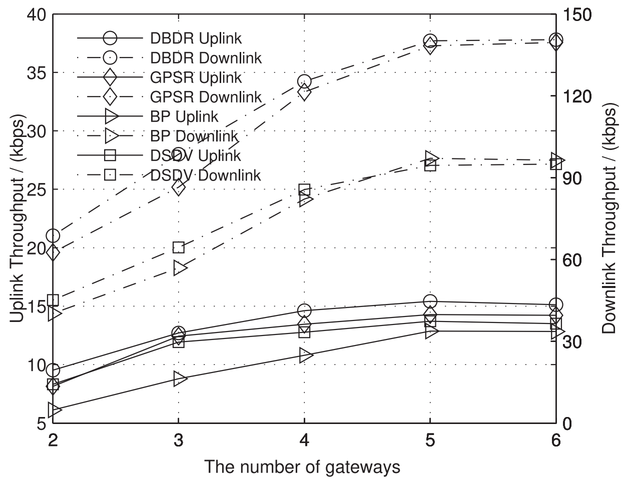

Fig. 10. Throughput of the routing protocols with different numbers of IGWs.

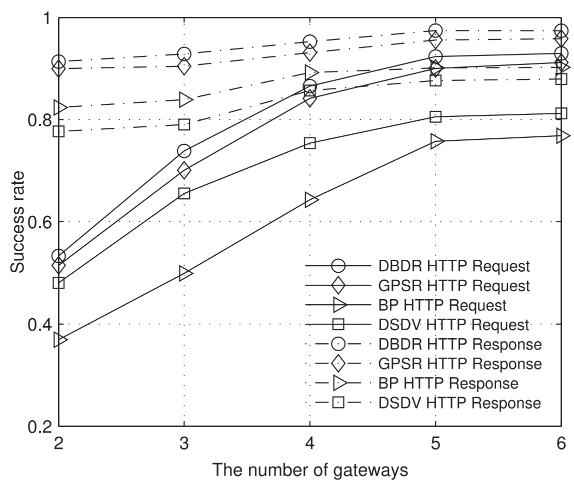

Fig. 11. HTTP request and response success rates of the routing protocols with different numbers of IGWs.

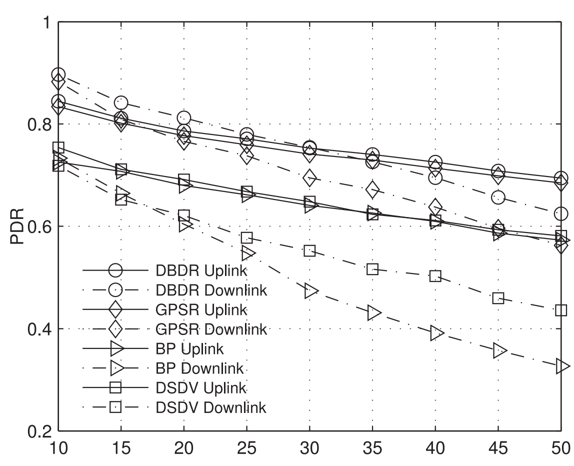

Fig. 12. PDRs of the routing protocols with different HTTP connection rates.

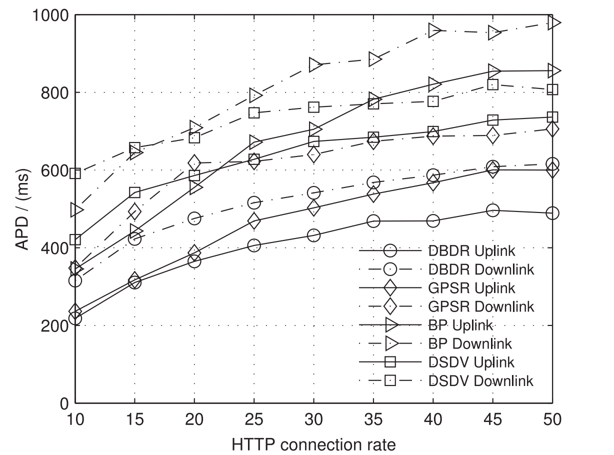

Fig. 13. APDs of the routing protocols with different HTTP connection rates.

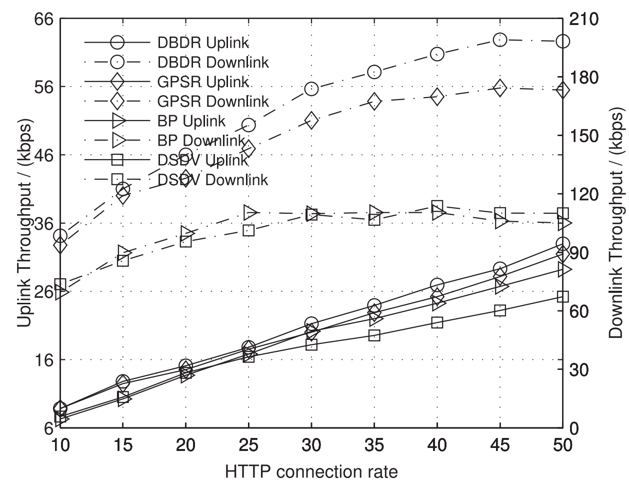

Fig. 14. Throughput of the routing protocols with different HTTP connection rates.

the network and will result in packet losses when the traffic loads approach the capacity. The severe channel competition and transmission collisions will also decrease PDR. The congested node will lead to a large backlog differential between its neighboring nodes. DBDR prioritizes the congested nodes and links in queue and link scheduling based on (5) and (7). Thus, the congestion- and distance-aware DBDR can relieve the network congestion and achieve the highest PDR.

Forwarding along the shortest path will lead to a low APD. However, the congestion in the shortest path will incur more queueing and channel access delay, thus resulting in a large APD. In this sense, it is shown in Fig. 13 that the congestion- and distance-aware DBDR outperforms the other three protocols in terms of APD.

With the highest PDR and the lowest APD, it is not a surprise that DBDR achieves the highest throughput, as shown in Fig. 14. Particularly, DBDR achieves a much higher downlink throughput than BP, DSDV and GPSR as the HTTP connection rate increases, which is important for the asymmetric Internet traffic.

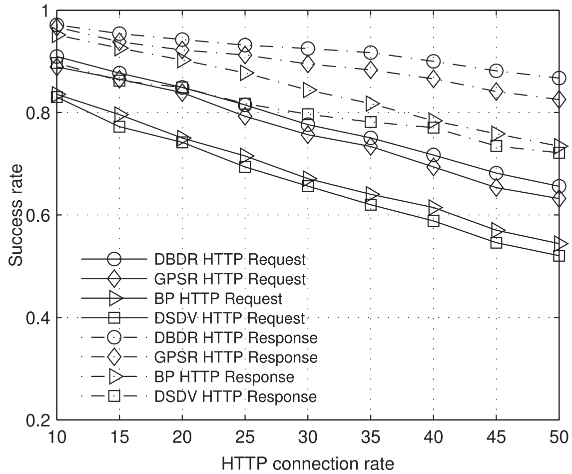

Fig. 15. HTTP request and response success rates of the routing protocols with different HTTP connection rates.

The success rates of HTTP requests/responses of DBDR are always higher than those of BP, DSDV and GPSR, although the increasing of HTTP connection rate makes the network getting congested, as shown in Fig. 15.

VII. Conclusion

To enable the future intelligent transportation system (ITS), this paper has studied the dynamic routing in vehicular ad hoc networks (VANETs) to implement Internet of Vehicles (IoV). We have proposed a distance-weighted back-pressure dynamic routing (DBDR), which is jointly designed with multi-hop Internet gateway discovery and vehicle mobility management for the Internet services. We also have proved the network stability property of DBDR using Lyapunov drift theory. The simulations are carried out in NS-2 and VanetMobiSim on a practical road scenario. The results show the performance improvement in terms of packet delivery ratio, end-to-end throughput and delay, and success rate for HTTP connections.

References

[1] A. K. Ligo and J. M. Peha, "Cost-effectiveness of sharing roadside infrastructure for Internet of Vehicles," *IEEE Trans. Intell. Transp. Syst.*, vol. 19, no. 7, pp. 2362–2372, Jul. 2018.

[2] S. A. Kazmi *et al.*, "Infotainment enabled smart cars: A joint communication, caching, and computation approach," *IEEE Trans. Veh. Technol.*, vol. 68, no. 9, pp. 8408–8420, Sep. 2019.

[3] J. Contreras-Castillo, S. Zeadally, and J. A. Guerrero-Ibañez, "Internet of Vehicles: Architecture, protocols, and security," *IEEE Internet Things J.*, vol. 5, no. 5, pp. 3701–3709, Apr. 2017.

[4] S. Sharma and B. Kaushik, "A survey on Internet of Vehicles: Applications, security issues & solutions," *Veh. Commun.*, vol. 20, no. 9, pp. 1–44, 2019.

[5] O. Senouci, Z. Aliouat, and S. Harous, "MCA-V2I: A multi-hop clustering approach over vehicle-to-internet communication for improving VANETs performances," *Future Gener. Comput. Syst.*, vol. 96, pp. 309–323, 2019.

[6] R. F. Atallah, M. J. Khabbaz, and C. M. Assi, "Modeling and performance analysis of medium access control schemes for drive-thru internet access provisioning systems," *IEEE Trans. Intell. Transp. Syst.*, vol. 16, no. 6, pp. 3238–3248, Dec. 2015.

[7] A. Baiocchi and F. Cuomo, "Infotainment services based on push-mode dissemination in an integrated VANET and 3G architecture," *J. Commun. Netw.*, vol. 15, no. 2, pp. 179–190, 2013.

[8] D. Abada and A. Massaq, "Improving relay selection scheme for connecting VANET to Internet over IEEE 802.11 p," *Int. J. Comput. Appl.*, vol. 132, no. 2, pp. 1–8, 2015.

[9] H. A. Omar, W. Zhuang, and L. Li, "On multihop communications for in-vehicle Internet access based on a TDMA MAC protocol," in *Proc. IEEE INFOCOM 2014*, Toronto, Ontario, Canada, pp. 1770–1778, 2014.

[10] A. Benslimane, S. Barghi, and C. Assi, "An efficient routing protocol for connecting vehicular networks to the Internet," *Pervasive Mobile Comput.*, vol. 7, no. 1, pp. 98–113, 2011.

[11] V. Sandonis, I. Soto, M. Calderon, and M. Urueña, "Vehicle to Internet communications using the ETSI ITS GeoNetworking protocol," *Trans. Emerg. Telecommun. Technol.*, vol. 27, no. 3, pp. 373–391, 2016.

[12] J. Cheng, J. Cheng, M. Zhou, F. Liu, S. Gao, and C. Liu, "Routing in Internet of Vehicles: A review," *IEEE Trans. Intell. Transp. Syst.*, vol. 16, no. 5, pp. 2339–2352, Oct. 2015.

[13] C. E. Perkins, E. M. Royer, and S. Das, "Ad-hoc on-demand distance vector (AODV) routing," *IETF RFC 3561*, 2003.

[14] D. Johnson, Y. Hu, and D. Maltz, "The dynamic source routing protocol (DSR) for mobile ad hoc networks for IPv4," *IETF RFC 4728*, 2007.

[15] C. E. Perkins and P. Bhagwat, "Highly dynamic destination-sequenced distance-vector routing (DSDV) for mobile computers," *SIGCOMM Comput. Commun. Rev.*, vol. 24, no. 4, pp. 234–244, Oct. 1994.

[16] A. Ullah, X. Yao, S. Shaheen, and H. Ning, "Advances in position based routing towards ITS enabled FoG-oriented VANET: A survey," *IEEE Trans. Intell. Transp. Syst.*, vol. 21, no. 2, pp. 828–840, Feb. 2020.

[17] Y. Wu, Y. Zhu, and Bo Li, "Trajectory improves data delivery in vehicular networks," in *Proc. IEEE INFOCOM 2011*, Shanghai, China, pp. 2183–2191, Apr. 2011.

[18] Z. Liu, T. Zhao, W. Yan, and X. Li, "GOSR: Geographical opportunistic source routing for vanets," *ACM SIGMOBILE Mobile Comput. Commun. Rev.*, vol. 13, no. 1, pp. 48–51, Jun. 2009.

[19] I. Leontiadis and C. Mascolo, "Geopps: Geographical opportunistic routing for vehicular networks," in *Proc. IEEE Int. Symp. World Wireless, Mobile Multimedia Netw.*, Espoo, Finland, Jun. 2007, pp. 1–6.

[20] B. Karp and H. T. Kung, "GPSR: Greedy perimeter stateless routing for wireless networks," in *Proc. ACM MOBICOM*, Boston, MA, USA, 2000, pp. 243–254.

[21] Y. Wu, Y. Zhu, and B. Li, "Infrastructure-assisted routing in vehicular networks," in *Proc. IEEE INFOCOM*, Orlando, FL, USA, Mar. 2012, pp. 1485–1493.

[22] L. Zhang, W. Cao, X. Zhang, and H. Xu, "MAC2: Enabling multicasting and congestion control with multichannel transmission for intelligent vehicle terminal in Internet of Vehicles," *Int. J. Distrib. Sensor Netw.*, vol. 14, no. 8, pp. 1485–1493, 2018.

[23] N. Li, J. Martnez-Ortega, V. H. Daz, and J. A. S. Fernandez, "Probability prediction-based reliable and efficient opportunistic routing algorithm for vanets," *IEEE/ACM Trans. Netw.*, vol. 26, no. 4, pp. 1933–1947, Aug. 2018.

[24] L. Tassiulas and A. Ephremides, "Stability properties of constrained queueing systems and scheduling policies for maximum throughput in multihop radio networks," *IEEE Trans. Autom. Control*, vol. 37, no. 12, pp. 1936–1948, Dec. 1992.

[25] M. J. Neely, E. Modiano, and C. E. Rohrs, "Dynamic power allocation and routing for time varying wireless networks," *IEEE J. Sel. Areas Commun.*, vol. 23, no. 1, pp. 89–103, Jan. 2005.

[26] M. H. Homaei, F. Soleimani, S. Shamshirband, A. Mosavi, N. Nabipour, and A. R. Vrkonyi-Kczy, "An enhanced distributed congestion control method for classical 6lowpan protocols using fuzzy decision system," *IEEE Access*, vol. 8, pp. 20 628–20 645, Jan. 2020.

[27] T. Qiu, R. Qiao, and D. O. Wu, "EABS: An event-aware backpressure scheduling scheme for emergency Internet of Things," *IEEE Trans. Mobile Comput.*, vol. 17, no. 1, pp. 72–84, Jan. 2018.

[28] C. Makaya and S. Pierre, "An architecture for seamless mobility support in ip-based next-generation wireless networks," *IEEE Trans. Veh. Technol.*, vol. 57, no. 2, pp. 1209–1225, Mar. 2008.

[29] J. Lloret, A. Canovas, A. Catalá, and M. Garcia, "Group-based protocol and mobility model for VANETs to offer internet access," *J. Netw. Comput. Appl.*, vol. 36, no. 3, pp. 1027–1038, 2013.

[30] A. Benslimane, T. Taleb, and R. Sivaraj, "Dynamic clustering-based adaptive mobile gateway management in integrated VANET 3G heterogeneous wireless networks," *IEEE J. Sel. Areas Commun.*, vol. 29, no. 3, pp. 559–570, Mar. 2011.

[31] T. Bellache, S. Kallel, O. Shagdar, and S. Tohme, "GeoMIP: A novel mobility management solution for Internet and VANET communication using geographic partition in mobile IP," in *Proc. Wireless Days (WD)*, Dubai, UAE, 2018, pp. 21–27.

[32] M. Bechler and L. Wolf, "Mobility management for vehicular ad hoc networks," in *Proc. IEEE Veh. Technol. Conf.*, Dallas, TX, USA, 2005, pp. 2294–2298.

[33] M. T. Abbas, A. Muhammad, and W.-C. Song, "SD-IoV: SDN enabled routing for Internet of Vehicles in road-aware approach," *J. Ambient Intell. Humanized Comput.*, vol. 11, no. 3, pp. 1265–1280, 2020.

[34] O. S. Al-Heety, Z. Zakaria, M. Ismail, M. M. Shakir, S. Alani, and H. Alsariera, "A comprehensive survey: Benefits, services, recent works, challenges, security, and use cases for SDN-VANET," *IEEE Access*, vol. 8, pp. 91 028–91 047, 2020.

[35] K. Smida, H. Tounsi, M. Frikha, and Y. Song, "Software defined Internet of Vehicles: A survey from qos and scalability perspectives," in *Proc. 15th Int. Wireless Commun. Mobile Comput. Conf. (IWCMC)*, Tangier, Morocco, 2019, pp. 1349–1354.

[36] J. Lu, Z. Huang, N. Liu, and Q. Guan, "Distance-weighted backlog differentials for back-pressure routing in multi-hop wireless networks," in *Proc. IEEE ICCC*, Shanghai, China, 2014, pp. 791–795.

[37] T. Issariyakul and E. Hossain, *Introduction to Network Simulator 2 (NS2)*. Boston, MA, USA: Springer, 2009.

[38] J. Härri, F. Filali, C. Bonnet, and M. Fiore, "Vanetmobisim: Generating realistic mobility patterns for VANETs," in *Proc. 3rd Int. Workshop Veh. Ad Hoc Netw.*, Los Angeles, CA, USA, 2006, pp. 96–97.

[39] Q. Guan, F. R. Yu, S. Jiang, and G. Wei, "Prediction-based topology control and routing in cognitive radio mobile ad hoc networks," *IEEE Trans. Veh. Technol.*, vol. 59, no. 9, pp. 4443–4452, Nov. 2010.

[40] A. A. Ba, A. Hafid, and J. Drissi, "Broadcast control-based routing protocol for Internet access in VANETs," in *Proc. IEEE Int. Wireless Commun. Mobile Comput. Conf.*, Istanbul, Turkey, 2011, pp. 1766–1771.

[41] C. Cooper, D. Franklin, M. Ros, F. Safaei, and M. Abolhasan, "A comparative survey of VANET clustering techniques," *IEEE Commun. Surv. Tut.*, vol. 19, no. 1, pp. 657–681, 2017.

[42] X. Zhang, X. Cao, L. Yan, and D. K. Sung, "A street-centric opportunistic routing protocol based on link correlation for urban VANETs," *IEEE Trans. Mobile Comput.*, vol. 15, no. 7, pp. 1586–1599, Jul. 2016.

[43] K. Abrougui, A. Boukerche, and R. W. N. Pazzi, "Location-aided gateway advertisement and discovery protocol for VANETs," *IEEE Trans. Veh. Technol.*, vol. 59, no. 8, pp. 3843–3858, Oct. 2010.

[44] T. Liu, Y. Zhu, R. Jiang, and Q. Zhao, "Distributed social welfare maximization in urban vehicular participatory sensing systems," *IEEE Trans. Mobile Comput.*, vol. 17, no. 6, pp. 1314–1325, Jun. 2018.

[45] L. Wu, Y. Xia, Z. Wang, and H. Wang, "Be stable and fair: Robust data scheduling for vehicular networks," *IEEE Access*, vol. 6, pp. 32 839–32 849, 2018.

[46] X. Meng, J. Lv, and S. Ma, "Applying improved k-means algorithm into official service vehicle networking environment and research," *Soft Comput.*, vol. 24, no. 11, pp. 8355–8363, 2020.

[47] Y. Peng and J. M. Chang, "A novel mobility management scheme for integration of vehicular ad hoc networks and fixed ip networks," *Mobile Netw. Appl.*, vol. 15, no. 1, pp. 112–125, 2010.

[48] Y. Bi, H. Zhou, W. Xu, X. S. Shen, and H. Zhao, "An efficient PMIPv6-based handoff scheme for urban vehicular networks," *IEEE Trans. Intell. Transp. Syst.*, vol. 17, no. 12, pp. 3613–3628, Dec. 2016.

[49] IEEE Standards Association, "Wireless LAN medium access control (MAC) and physical layer (PHY) specifications: Amendment 6: Wireless access in vehicular environments," *IEEE Standard 802.11p*, 2010.

[50] C. Perkins, "IP mobility support for IPv4," *IETF RFC 5944*, Nov. 2010.

[51] L. Georgiadis, M. J. Neely, and L. Tassiulas, *Resource Allocation and Cross-Layer Control in Wireless Networks*. (Foundations & Trends in Networking). Netherlands: Now, 2006.

Ruiyan Han received the B.S. degree from Harbin Normal University, Harbin, China, in 2013, and the M.S. degree from Yunnan Minzu University, Kunming, China, in 2016. She is currently working toward the Ph.D. degree with the School of Electronic and Information Engineering, South China University of Technology, Guangzhou, China. Her current research interests include vehicular ad hoc networks and wireless sensor networks.

Quansheng Guan (Senior Member, IEEE) received the Ph.D. degree from the South China University of Technology (SCUT) in 2011. From 2009 to 2010, he was a Visiting Ph.D. Student with the University of British Columbia, Canada. From 2012 to 2013, he was a Postdoc Researcher with the Chinese University of Hong Kong. He was a Visiting Scholar with the Singapore University of Technology and Design in 2013, and a Visiting Professor with Polytech Nantes, France, in 2016. He is currently a Full Professor with the School of Electronic and Information Engineering, SCUT. His main research interests include wireless networks, underwater acoustic networks, as well as cloud/fog computing.

Dr. Guan was the co-recipient of the Best Paper Awards from IEEE ICCC 2014 and IEEE ICNC 2016, and the Best Demo Award from ACM WUWNET 2018. He is an Associate Editor for IEEE ACCESS, *International Journal of Distributed Sensor Networks*, and a Guest Editor for *Mobile Information System*.

F. Richard Yu (Fellow, IEEE) received the Ph.D. degree in electrical engineering from the University of British Columbia (UBC) in 2003. From 2002 to 2006, he was with Ericsson, Lund, Sweden, and a start-up in California, USA. In 2007, he joined Carleton University, where he is currently a Professor. His research interests include connected/autonomous vehicles, security, artificial intelligence, distributed ledger technology, and wireless cyber-physical systems. He received the IEEE TCGCC Best Journal Paper Award in 2019, the Distinguished Service Awards in 2019 and 2016, the Outstanding Leadership Award in 2013, the Carleton Research Achievement Awards in 2012 and 2020, the Ontario Early Researcher Award (formerly Premiers Research Excellence Award) in 2011, the Excellent Contribution Award at IEEE/IFIP TrustCom 2010, the Leadership Opportunity Fund Award from Canada Foundation of Innovation in 2009, and the Best Paper Awards at IEEE ICNC 2018, VTC 2017 Spring, ICC 2014, Globecom 2012, IEEE/IFIP TrustCom 2009, and International Conference on Networking 2005.

He is on the editorial boards of several journals, including Co-Editor-in-Chief for *Ad Hoc & Sensor Wireless Networks*, Lead Series Editor for the IEEE TRANSACTIONS ON VEHICULAR TECHNOLOGY, IEEE COMMUNICATIONS SURVEYS & TUTORIALS, and IEEE TRANSACTIONS ON GREEN COMMUNICATIONS AND NETWORKING. He was the Technical Program Committee (TPC) Co-Chair of numerous conferences. He has been named in the Clarivate Analytics list of "Highly Cited Researchers" since 2019. He is an IEEE Distinguished Lecturer of both Vehicular Technology Society (VTS) and Communications Society. He is an elected member of the Board of Governors of the IEEE VTS and Editor-in-Chief for IEEE VTS *Mobile World Newsletter*. He is a registered Professional Engineer in the province of Ontario, Canada, an IET Fellow, and Engineering Institute of Canada (EIC) Fellow.

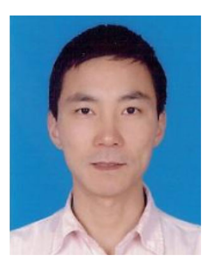

Jinglun Shi received the B.S., M.S., and Ph.D. degrees from the School of Electronic and Information Engineering, South China University of Technology (SCUT), in 1999, 2000, and 2004, respectively. Before joining SCUT, he was a Postdoctoral Research Associate with Seoul National University. During his graduate program, he was a Research Fellow with Hong Kong Baptist University and Torento University. His research interests include wireless sensor networks, exoskeleton robot, and artificial intelligence.

Fei Ji (Member, IEEE) received the Ph.D. degree from the South China University of Technology (SCUT) in 1998. Upon graduation, she joined SCUT as a Lecturer. From 2003 to 2008, she was an Associate Professor. From 2001 to 2002, she was with the City University of Hong Kong as a Research Assistant and from 2005 to 2005, a Senior Research Associate. From 2009 to 2010, she was with the University of Waterloo as a Visiting Scholar. She is currently a Full Professor with SCUT. Her research interests include wireless communication system and networking.